# Road-Crossing Assistance by Traffic Flow Analysis

Adi Perry and Nahum Kiryati

School of Electrical Engineering
Tel Aviv University
Ramat Aviv 69978, Israel

**Abstract.** We present a system to alert visually impaired pedestrians of vehicles approaching a road-crossing without traffic control. The system is computationally efficient, requires low-cost hardware, and can be mounted on existing street infrastructure, such as sign or lighting poles. The incoming video stream, showing the approaching traffic, is transformed to a one-dimensional signal, that is forwarded to a decision module. Preliminary experimental results indicate promising probability-of-detection and false alarm rates, while providing sufficiently early warning to the pedestrian. The planned target hardware is a solar-charged low cost Android device.

**Keywords:** road crossing assistance, approaching traffic analysis, optic flow, blind, visually impaired, resource-limited system

## 1 Introduction

For visually impaired pedestrians, crossing a street in the absence of traffic control is a challenge. Drivers do not reliably yield to pedestrians, even those who are clearly visual impaired (holding a white cane), requiring pedestrians to cross in traffic gaps [6]. To identify traffic gaps, visually impaired pedestrians rely on hearing. The common strategy is "cross when quiet" [14]. However, relying on early detection of vehicle noise is risky, especially since the low noise level of modern cars can easily be masked by background noise. Furthermore, pedestrians with less than perfect hearing cannot follow the "cross when quiet" rule.

US data [2] indicates that the average crossing speed is 4 feet (about 1.2m) per second. A standard urban one-way single-lane street with two shoulders is 18 feet (5.5m) wide and takes 4.5 seconds to cross. A standard two-way street or one-way with two lanes is 28 feet (8.5m) wide, taking 7 seconds to cross. The traffic gap must be longer than these figures, and for safe crossing an advance warning of at least 7 seconds is necessary.

Pun *et al* [13] reviewed the field of assistive devices, especially those that use image and video processing to convert visual data to another modality, such as auditory or haptic, which can be delivered to the blind person. Several systems help locating and identifying points of interest [5] and road crossings [16, 9]. Other devices provide auditory or other indications regarding traffic light

status [3, 4]. "Smart canes", employing various types of sensors, have been suggested [10, 1, 7], but are intended primarily for short-range obstacle detection and navigation. All these systems do not address the fundamental difficulty of crossing a road in the absence of traffic control.

An ideal solution to the road-crossing problem must reliably analyze traffic flow, detect traffic gaps, and be sufficiently robust to operate at a variety of weather conditions, day and night. Moreover, it has to be easy and cheap to install, operate and maintain. This work is intended to be a first step towards meeting this challenge.

We present a low-cost system to detect and alert pedestrians of vehicles approaching a crosswalk. When fully developed, it will be possible to mount the system on existing street infrastructure, such as traffic signs or illumination poles. The system adapts to the scene, thus minimizing installation and maintenance effort. It can detect approaching vehicles well before they reach the road crossing, thus indicating traffic gaps that are sufficient for safe crossing.

## 2 Hardware Platform & Installation

The input device is a video camera, capturing the incoming traffic, as illustrated in Fig. 1. The video signal is processed by low cost, lightweight computing hardware, that eventually generates the indication signal.

The hardware platform can include a compact solar panel and a rechargeable battery, to allow autonomous operation without reliance on the electric power grid. This can enhance the applicability of the system, and reduce its installation and maintenance costs. A block diagram of the system is shown in Fig. 2.

Indication of incoming traffic, or lack thereof, can be delivered to the user as an audio or tactile signal, or via a local networking interface (such as Bluetooth or WLAN) to a smartphone or a dedicated receiver.

We developed the system on a standard laptop PC, with a modified Logitech QuickCam 9000 WebCam. Targeting a low-cost solution, we implemented the algorithm as a cross-platform code, and tested it on BeagleBoard xM hardware, an open-source platform consisting of TI's OMAP 3530 (ARM processor + DSP),

Fig. 1: Mounting the system on a sign or lighting pole near a road crossing, with the camera facing the approaching traffic.

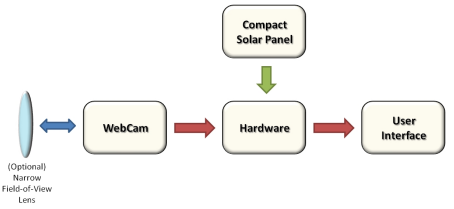


Fig. 2: The system consists of a low cost camera, streaming video to a computing device, possibly powered by a compact solar panel. User interaction options range from an auditory or visual alert to communication via a local area or cellular network. A narrow field of view lens can be used to improve the observability of distant vehicles.

suitable for rapid prototyping. With the proliferation of low-cost Android devices with built-in cameras, we are currently porting the system to Android OS.

## 3 Algorithm

We examined various approaches for efficient detection and evaluation of approaching traffic on a resource-limited platform. A generic approach that comes to mind is detecting any new object appearing in the field of view, tracking it, analyzing its motion and estimating its *Time to Contact* (TTC) as the basis for issuing an alert. Lee [11] observed that in a simple but typical case, the TTC can be estimated based on the incoming object's expansion rate, measured in the image plane. A newer approach for TTC estimation [8] treats the approaching vehicle as a moving plane.

In our application, the field of view (FOV) of the camera should be sufficiently wide to capture nearby vehicles (possibly leaving a parking spot). However, most approaching vehicles first appear as tiny spots near the vanishing point (VP)[1] Given the limited pixel-count of low cost video cameras, the wide FOV implies that the spatial resolution near the vanishing point is quite low. These constraints imply that the main challenge is early detection of the incoming vehicle, meeting the advance warning time requirement. Therefore, in most cases precise TTC estimation is not the issue. Also note that the approximations on which TTC algorithms rely do not hold at the most significant moment, when the vehicle is seen as a tiny, far-away spot.

We convert the space-time video processing problem to a 1-D signal analysis problem, by computing a scalar motion measure, referred to as *Activity*, reflecting the entire *relevant* motion in the scene. Objects moving along the road towards the camera induce pulses in the Activity signal, such that a significant rising Activity slope suggests an approaching vehicle. Early detection of approaching vehicles with few false alarms amounts to discrimination between a true rising Activity slope and random noise and clutter in the Activity signal.

[1] We use the term *vanishing point* in a loose sense, including the case of a curved road.

### 3.1 Activity Estimation

Brightness patterns in the image move as the objects that give rise to them move in the scene, leading to optical flow. We estimate the optical flow using a computationally-efficient version of a non-iterative sparse Lucas-Kanade [12] algorithm. The estimation errors typical to the Lucas-Kanade method can be tolerated in our application; as will be seen, the activity signal, derived from the optical flow, is an integral measure in which these errors are spatially averaged over parts of the image domain.

We employ integral images to improve the efficiency of the algorithm, as proposed by Senst *et al* [15], calculating integral versions of the gradient products of the image $I_x \cdot I_x,\ I_x \cdot I_y,\ I_y \cdot I_y$ and $I_x \cdot I_t,\ I_y \cdot I_t$. Evaluating a structure tensor (or a covariance matrix) is required for estimating each flow vector in the Lucas-Kanade algorithm, and each of its matrix elements can be efficiently evaluated using four simple arithmetic operations, regardless of the neighborhood size that is taken into account.

Parts of the optical flow field are associated with risk-posing approaching vehicles. Other parts might reflect distancing traffic on another lane, pedestrians crossing the road, and movements due to wind or camera vibrations. The proposed activity measure $A(t)$ is obtained by projecting the optical flow field $\boldsymbol{u}(x, y; t)$ onto a *projection map*. The projection map $\boldsymbol{m}(x, y)$ is a vector field supported on image regions corresponding to lanes carrying traffic towards the camera, each vector representing the local direction of approaching traffic. Formally,

$$A(t) = \sum_{x,y} \boldsymbol{m}(x, y) \cdot \boldsymbol{u}(x, y; t). \tag{1}$$

The scalar, time-dependent Activity is fast to compute, and quantifies the entire risk-inducing motion in the scene.

Assuming a one-way road, the projection map can be automatically generated by temporal averaging of the optical flow over a training period, see Fig. 3. The averaging process cancels the randomly oriented contributions that are due to vibrations, wind and similar phenomena, while highlighting the consistent, dominant, risk-inducing traffic motion directions in the road area alone. Slight adaptation of this procedure is necessary for dealing with two-way roads, where consistent distancing traffic is also expected within the visual field of the camera.

**Variable density & spatially weighted optical flow computation:** Maintaining minimal system cost calls for resource-limited hardware. Since optical flow computation is the most demanding element in the proposed algorithm, it is most lucrative for streamlining and optimization. Typically, large parts of the field of view, such as sidewalks and background structures, do not hold risk-posing motion. These regions, once determined, might be excluded from optical flow estimation altogether. In image regions corresponding to nearby parts of the scene, where vehicles appear quite large and expand substantially, spatially-sparse optical flow computation might be sufficient. Conversely, high density optical flow computation can be called for just where necessary, near the vanishing

point, where approaching vehicles first appear as tiny spots. These considerations can be readily represented by the automatically-generated projection map. Furthermore, the *magnitude* of the projection-map vectors can be modified to emphasize motion near the vanishing point, thus improving the warning time see an example in Fig. 4. Note that the vanishing point can be readily detected during training, by back-tracking the projection-map vectors to the source of the flow.

### 3.2 Detecting Approaching Vehicles

In certain applications, the raw Activity signal can be delivered to the pedestrian in analog form, leaving the actual decision regarding road crossing safety in the human domain. However, in most cases we wish to provide the pedestrian with a binary signal, suggesting either that traffic is approaching ('TRAFFIC' state) or that a sufficient traffic gap occurs at that moment ('GAP' state).

Despite the substantial SNR in the Activity signal near Activity peaks, *early* detection of an approaching vehicle, at the early rising stage of the corresponding activity pulse, when the SNR is poor, is not easy. Note that the pulse shape and magnitude are generally not known in advance, as they depend on the particular vehicle characteristics, as well as on the specific scene structure and viewing conditions.

Robust detection cannot be accomplished by simple thresholding of the Activity signal; the signal should be examined within a sliding temporal window. This improves the effective SNR, the detection probability and the false alarm rate, at the cost of increased detection latency. The sliding window must therefore be short enough to maintain the warning time necessary for safe road crossing.

(a) (b)

Fig. 3: Projection map, obtained by temporal averaging of the optical flow field over a training period. (3a) Sparse vector-field display. (3b) The flow direction in each pixel is mapped to hue, the magnitude to saturation. The color key is shown top-right.

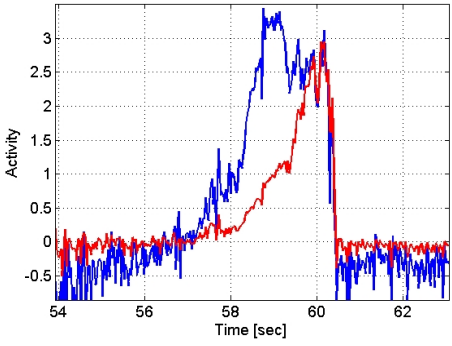


Fig. 4: Activity signal corresponding to an approaching vehicle, with (blue) and without (red) emphasizing the projection map magnitude near the vanishing point.

Assume that the complete Activity pulse length is $L$; we wish to detect the presence of the pulse after $N \leq L$ samples are acquired. The warning is therefore delayed by $N$ samples with respect to the first appearance of the approaching vehicle.

Within the temporal window of size $N$, suppose that there is either a traffic gap, such that the Activity is $A(n) = v(n)$, where $v(n)$ is a random noise process, or a vehicle initially appears, so $A(n) = s(n)+v(n)$, where $s(n)$ is the pulse shape corresponding to the specific vehicle and viewing conditions, referred to as the rising pulse. Temporal windows corresponding to earlier or later appearance of a vehicle are discussed in the sequel.

We formulate the 'TRAFFIC' and 'GAP' state hypotheses as follows:

$$\begin{array}{ll} H_1: & A(n) = s(n) + v(n) \quad A(n) \sim \mathcal{N}\left(s(n), \sigma^2\right) \\ H_0: & A(n) = v(n) \quad\quad\quad\quad\;\; A(n) \sim \mathcal{N}\left(0, \sigma^2\right) \end{array} \tag{2}$$

where $A(n)$ is the Activity measurement and $v(n)$ is modelled as zero-mean additive white Gaussian noise (AWGN): $v(n) \sim \mathcal{N}\left(0, \sigma^2\right)$.

The samples $A(n)$ inside a sliding window of length $N$ can be represented as a Gaussian random vector $\underline{y}$, with the following likelihood functions:

$$\begin{aligned} f_y(\underline{y}|\theta_1) &= \frac{1}{(2\pi)^{N/2}\sigma^N} \prod_{n=0}^{N-1} exp\left(-\frac{(a_n - s_n)^2}{2\sigma^2}\right) \\ f_y(\underline{y}|\theta_0) &= \frac{1}{(2\pi)^{N/2}\sigma^N} \prod_{n=0}^{N-1} exp\left(-\frac{a_n^2}{2\sigma^2}\right) \end{aligned} \tag{3}$$

where we replaced the notations $A(n), S(n)$ by $a_n, s_n$. Applying a Likelihood Ratio Test for discriminating between the two hypotheses

$$LRT = \frac{\frac{1}{(2\pi)^{N/2}\sigma^N}\prod_{n=0}^{N-1} exp\left(-\frac{(a_n-s_n)^2}{2\sigma^2}\right)}{\frac{1}{(2\pi)^{N/2}\sigma^N}\prod_{n=0}^{N-1} exp\left(-\frac{a_n^2}{2\sigma^2}\right)} \gtrless \lambda \tag{4}$$

where $\lambda$ is a discriminative threshold, leads to the detection rule:

$$\sum_{n=0}^{N-1} a_n s_n \gtrless \frac{1}{2}\left(2\sigma^2 \ln\lambda + \sum_{n=0}^{N-1} s_n^2\right). \tag{5}$$

The left hand side describes a correlator of the input Activity with the rising pulse template, and the right hand side is an application-dependent threshold. For determining the threshold, we apply the Neyman-Pearson criterion, which sets the threshold to maintain a given false-alarm probability.

The left hand side is a random Gaussian variable with variance $\sigma^2 \sum_{n=0}^{N-1} s_n^2$, that we denote as $\tilde{y}$. The false-alarm probability is given by the tail distribution of the 'GAP' ($\theta_0$) hypothesis:

$$P_{FA} = \int_{\gamma}^{\infty} f_{\tilde{y}}(z|\theta_0)dz = Pr\left(\tilde{y} > \gamma|\theta_0\right) =$$
$$Pr\left(\frac{\tilde{y}}{\sigma\sqrt{\sum s_n^2}} > \gamma\frac{1}{\sigma\sqrt{\sum s_n^2}}\right) = Q\left(\frac{\gamma}{\sigma\sqrt{\sum s_n^2}}\right) = 1 - \phi\left(\frac{\gamma}{\sigma\sqrt{\sum s_n^2}}\right) \tag{6}$$

where $\phi(x)$ is the cumulative distribution function of the standard normal distribution and $Q(x)$ is its tail probability: $Q(x) = 1 - Q(-x) = 1 - \phi(x)$.

This yields a threshold $\gamma = Q^{-1}\left(P_{FA}\right)\sigma\sqrt{\sum s_n^2}$ which can be determined by the SNR and the acceptable false-alarm rate. The detector can be described as

$$D(a_0, ..., a_{N-1}) \equiv \frac{\sum_{n=0}^{N-1} a_n s_n}{\sum_{n=0}^{N-1} s_n^2} \gtrless Q^{-1}\left(P_{FA}\right)\sigma \tag{7}$$

which is familiar as the result of applying a matched filter, correlating the input measurements with the known signal that we wish to detect. The corresponding probability of detection is:

$$P_D = Pr\left(\tilde{y} > \gamma|\theta_1\right) = ... = Q\left(Q^{-1}\left(P_{FA}\right) - \frac{\sqrt{\sum s_n^2}}{\sigma}\right) \tag{8}$$

So far, we discussed the most challenging aspect of detection, the initial detection of an approaching vehicle. The detector is causal, hence the warning is delayed by $N$ samples. Since the rising pulse typically increases as the vehicle approaches, once the correlator crosses the threshold, it remains above it as long as the pulse rises. To maintain continuous detection of vehicles until they reach the crossing, we extend the correlator window size beyond $N$ as long as 'TRAFFIC' classifications are acquired, up to a maximal size not exceeding $L$. When vehicles appear late (e.g. leaving a parking spot close to the crossing), the rising pulse takes off at a rather high magnitude and the correlator immediately crosses the threshold.

### 3.3 Estimating Detector Parameters

The detector is parameterized by the noise variance (that can be estimated), and the expected shape of the activity pulse. During a training period, by the time the Projection Map is generated, the system produces Activity measurements. After sufficient training, the measurements are used to automatically generate the activity pulse model and estimate the noise variance.

The system scans the input signal acquired during training to locate its strongest local maxima, and crops a window of 10 seconds around each maximum, where most of the samples precede the maximum. The windows are batched together, and used to estimate the noise variance and activity pulse template. In practice, we model the rising pulse as the median of the cropped temporal windows. Fig. 5 illustrates the process.

## 4 Results

Fig. 6c shows snapshots from a day-time video sequence obtained by the system camera in a single-lane one-way street. Fig. 6a is the Activity signal corresponding to the same experimental session. Fig. 6b zooms on the time interval in which the snapshots shown in Fig. 6c were taken. The coloring of the graphs in Figs. 6a and 6b present the indication provided to the pedestrian, red meaning TRAFFIC and blue corresponding to GAP. As can be seen, TRAFFIC is declared 8-10 seconds before the vehicle reaches the camera, i.e., before the peak of the Activity signal, allowing safe crossing with substantial margin.

We recorded and annotated video taken from the system camera. For each vehicle, we noted its time of appearance $t_A$ and its time of disappearance $t_D$, and calculated its apparent time interval $T_{ap} = t_D - t_A$. Obviously, $T_{ap}$ sets an upper bound on the feasible warning time. The results were recorded with a modified USB camera and with an equivalent Point-and-Shoot camera. The USB camera is a standard webcam with its lens replaced to slightly narrow the field of view.

Ideally, a vehicle appears near the vanishing point, maximizing the feasible warning time. Note however that in certain urban or suburban scenes a vehicle can leave a parking spot within the field of view and close to the crossing, or

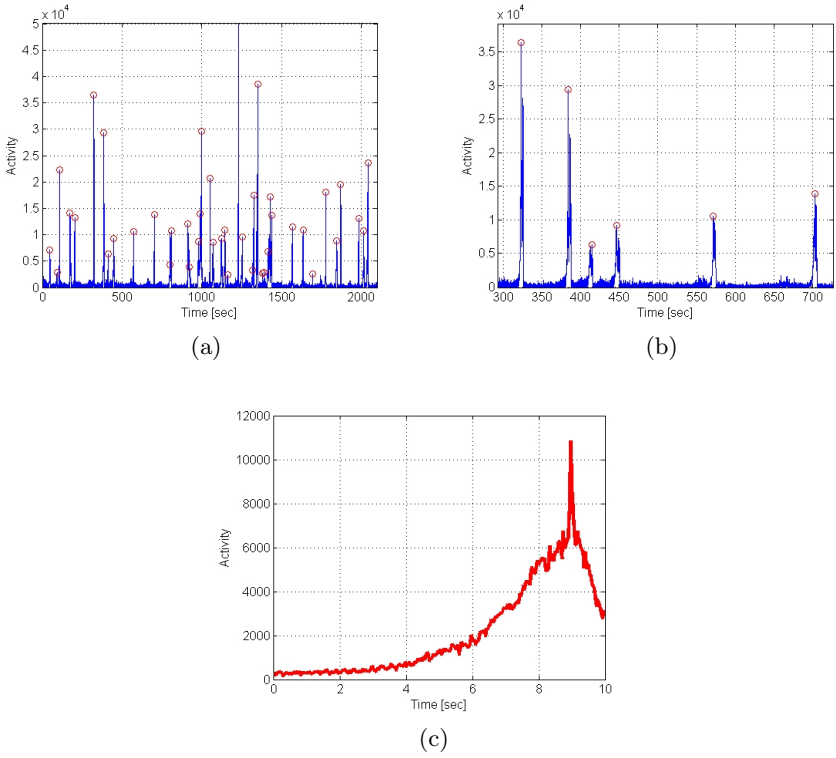


Fig. 5: Learning the activity pulse model
(5a) Activity signal over a 30 minutes training period, with the strongest local maxima detected. (5b) The same Activity results zoomed in for a few minutes of the training. (5c) The processed template that is used for correlation, generated as the median over the batch of windows.

might turn into the into the observed road from a nearby driveway. This means that while the apparent time $T_{ap}$ of each vehicle can be more than 10 seconds, which is more than enough; however, in certain cases $T_{ap}$ can be as short as one second, allowing neither the system nor a human observer an adequate warning period.

Fig. 7 presents typical results. The activity signal is shown as a function of time. It is colored black where there is no traffic, and the system declares no warning (true negative, TN). It is colored blue where the system detects genuine incoming traffic (true positive, TP). As can be seen, practically all vehicles are detected. However, the detector is necessarily causal, inducing some latency. The time interval between the first appearance of a vehicle and the initial warning is colored green (false negative, FN). At certain points, false alarms (false positive, FP) appear, colored red. Fig. 8 demonstrates false negative and false positive events that were encountered.

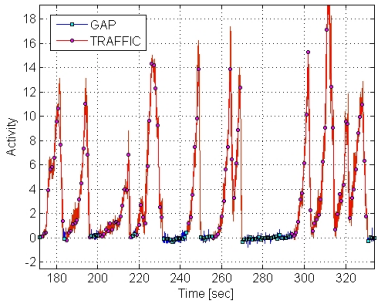


(a)

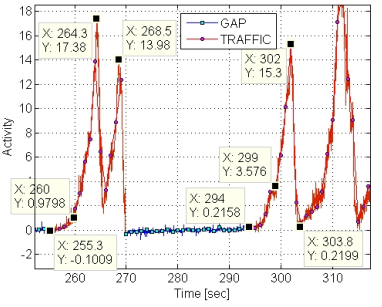


(b)


(c)

Fig. 6: Activity classification

(6a) Activity results for a typical scenario classified to TRAFFIC and GAP, colored red and blue respectively. (6b) The same Activity results expanded for a couple of approaching vehicles. (6c) Snapshots of the original video with time tags. The reader can observe that the TRAFFIC indication is declared very early, as soon as a vehicle appears.

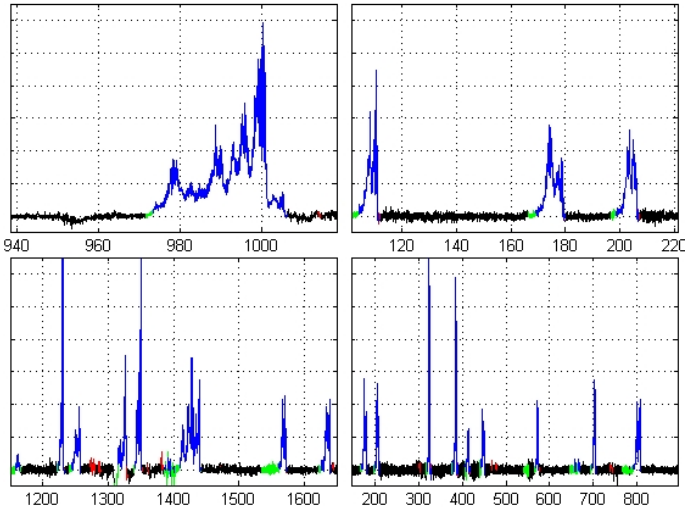


Fig. 7: Typical activity signal and classification of results
The plots describe the activity signal within four time intervals; time is labeled in seconds along the horizontal axis. The signal is colored according to the output of the system and the ground truth (true negative: black; true positive: blue; false negative: green; false positive: red).

For analysis, we executed the algorithm offline, on the recorded video, with various detector thresholds and settings. We register a single success per vehicle in case the detector issues a sufficiently early warning, meaning at most $\tau_{max}$ seconds after initial appearance *or* at least 7 seconds before reaching the crossing. The value $\tau_{max}$ corresponds to the window size $N$ (the minimal feasible warning time delay).

We constructed per-vehicle ROC curves based on comparison with the ground truth data. We calculate the True Positive Rate as the fraction of successes out of the total number of incoming vehicles:

$$TPR = \frac{TP}{TP + FN} = \frac{N_s}{N_{tot}} \tag{9}$$

where $N_s$ is the number of successes and $N_{tot}$ is the total number of vehicles. We calculate the False Positive Rate as

$$FPR = \frac{FP}{FP + TN} \tag{10}$$

where the values are previously defined and taken *per-sample* from the full recording. Note that defining the false positive rate per-sample is very severe, since even an isolated outlying false positive reading, that can easily be detected and eliminated without significant effect on the true positive rate, is registered.

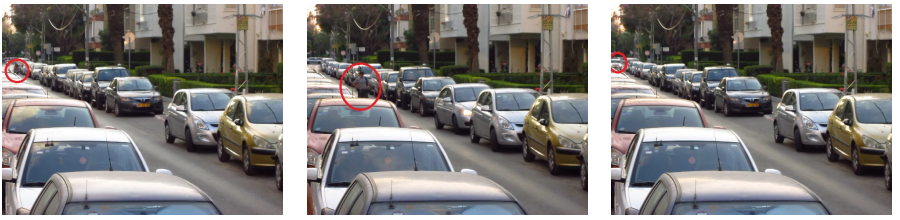

(a) (b) (c)

Fig. 8: Events giving rise to false positives (false alarms) and false negatives (8a) False negative corresponding to a slow, distant bicyclist. (8b) False positive induced by a person suddenly appearing in the road. (8c) False negative associated with a vehicle that appeared, stopped, and eventually turned right into a side street.

Fig. 9 presents a sample of analysis results. Fig. 9a shows the per-vehicle ROC curves for a few window sizes $N$, corresponding to 1 to 3 second durations. Fig. 9b is the histogram (distribution) of the advance warning times over 1 hour in a single-lane one-way street. The per-sample false positive level was set to 0.01 and only vehicles with $T_{ap}$ greater than 7 seconds are taken into account. Short warning times corresponded to slowly driving vehicles, including bicycles. By allowing a higher per-sample false positive level, most of the slow vehicles can be detected substantially earlier.

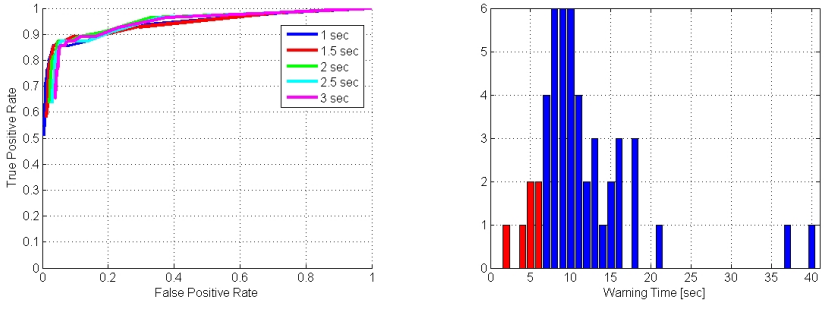


(a) (b)

Fig. 9: Analysis results
(9a) Per-vehicle ROC curves for a few window sizes $N$, corresponding to intervals between 1 second to 3 seconds. (9b) Warning times histogram covering 1 hour in a single-lane one-way street.

## 5 Discussion

We presented a computationally-lean system to detect and alert pedestrians of vehicles approaching a road-crossing. The system automatically adapts to the scene, and can be mounted on existing street infrastructure, facilitating simple installation. The system is designed primarily for blind and visually impaired people, but can potentially assist the young and the old, people with cognitive impairments, and others.

We implemented the system on a standard laptop PC, and also ported it on BeagleBoard xM hardware running Linux. An Android version using low-cost smartphone/tablet-like hardware is planned.

We tested the system at several locations, and achieved advance warning times approaching 9 seconds at typical day conditions with a rather wide field of view lens, slightly less at night scenarios. These results are promising, because a standard US two-lane street takes only about 7 seconds to cross. Night and poor weather conditions were examined succinctly and further experiments and analysis need to be conducted.

A single instance of the system is capable of detecting traffic approaching from a given direction and ignore distancing traffic. Full support of two-way traffic requires two instances of the system, mounted in opposite directions, preferably with a unified decision and pedestrian interface module.

Time to Contact (TTC) estimation, based on Horn *et al* [8], was also tested. As in our approach, it processes entire frames and yields a scalar signal, that could be considered as an alternative to the proposed Activity signal. The results were noisy and unstable compared to the results obtained using the suggested Activity measure.

Learning is an essential aspect of the system, including the generation of the projection map and the activity pulse model. The straightforward training and learning solutions employed in the current design leave room for sophisticated improvements.

The suggested approach is unique in being stationary and location-specific. The absence of ego-motion leads to a solution that is both robust and low-cost. Any person approaching the road crossing can take advantage of the system, with no need for a personally owned device such as a smartphone or a smart cane. This widens the potential reach of the system to weak parts of the society.

## References

1. Amedi, A.: Virtual cane for the visually impaired, presented at the international presidential conference. http://blog.imric.org/blog/sidney/virtual-cane-visually-impaired-presented-international-presidential-conference (June 2011)
2. American Association of State Highway and Transportation Officials: A Policy on geometric design of highways and streets. Washington, D.C. (2004)
3. Barlow, J., Bentzen, B., Tabor, L.: Accessible Pedestrian Signals: Synthesis and Guide to Best Practice. National Cooperative Highway Research Program (2003)

4. Bohonos, S., Lee, A., Malik, A., Thai, C., Manduchi, R.: Universal real-time navigational assistance (URNA): an urban bluetooth beacon for the blind. In: Proceedings of the 1st ACM SIGMOBILE international workshop on Systems and networking support for healthcare and assisted living environments. pp. 83–88. HealthNet '07, ACM, New York, NY, USA (2007)
5. Crandall, W., Bentzen, B., Myerss, L., Brabyn, J.: New orientation and accessibility option for persons with visual impairment: transportation applications for remote infrared audible signage. Clinical and Experimental Optometry 84, 120–131 (2001)
6. Emerson, R., Sauerburger, D.: Detecting approaching vehicles at streets with no traffic control. Journal of Visual Impairment & Blindness 102(12), 747 (2008)
7. Fallon, J.: Systems and methods for laser radar imaging for the blind and visually impaired (2008)
8. Horn, B., Fang, Y., Masaki, I.: Time to contact relative to a planar surface. In: Intelligent Vehicles Symposium, 2007 IEEE. pp. 68 –74 (June 2007)
9. Ivanchenko, V., Coughlan, J., Shen, H.: Crosswatch: A camera phone system for orienting visually impaired pedestrians at traffic intersections. In: Proceedings of the 11th international conference on Computers Helping People with Special Needs. pp. 1122–1128. ICCHP '08, Springer-Verlag, Berlin, Heidelberg (2008)
10. Kay, L.: A sonar aid to enhance spatial perception of the blind: engineering design and evaluation. Radio and Electronic Engineer 44 (1974)
11. Lee, D.: A theory of visual control of braking based on information about time-to-collision. Perception 5(4), 437–459 (1976)
12. Lucas, B., Kanade, T.: An iterative image registration technique with an application to stereo vision. In: Proceedings of the 7th International Joint Conference on Artificial Intelligence - Volume 2. pp. 674–679. Morgan Kaufmann Publishers Inc., San Francisco, CA, USA (1981)
13. Pun, T., Roth, P., Bologna, G., Moustakas, K., Tzovaras, D.: Image and video processing for visually handicapped people. J. Image Video Process. 2007, 4:1–4:12 (January 2007)
14. Sauerburger, D.: Developing criteria and judgment of safety for crossing streets with gaps in traffic. Journal of Visual Impairment & Blindness 93(7), 447–450 (1999)
15. Senst, T., Eiselein, V., Sikora, T.: II-LK - a real-time implementation for sparse optical flow. In: Proceedings of the 7th International Conference on Image Analysis and Recognition - Volume Part I. pp. 240–249. ICIAR'10, Springer-Verlag, Berlin, Heidelberg (2010)
16. Shioyama, T., Uddin, M.: Detection of pedestrian crossings with projective invariants from image data. Measurement Science and Technology 15(12), 2400 (2004)